Robust Sum-Rate Maximization in Transmissive RMS Transceiver-Enabled SWIPT Networks

Zhendong Li, Wen Chen, *Senior Member, IEEE*, Ziheng Zhang, Qingqing Wu, *Senior Member, IEEE*, Huanqing Cao, and Jun Li, *Senior Member, IEEE*

***Abstract*—In this article, we propose a state-of-the-art downlink communication transceiver design for transmissive reconfigurable metasurface (RMS)-enabled simultaneous wireless information and power transfer (SWIPT) networks. Specifically, a feed antenna is deployed in the transmissive RMS-based transceiver, which can be used to implement beamforming. According to the relationship between wavelength and propagation distance, the spatial propagation models of plane and spherical waves are built. Then, in the case of imperfect channel state information (CSI), we formulate a robust system sum-rate maximization problem that jointly optimizes RMS transmissive coefficient, transmit power allocation, and power splitting ratio design while taking account of the nonlinear energy harvesting model and outage probability criterion. Since the coupling of optimization variables, the whole optimization problem is nonconvex and cannot be solved directly. Therefore, the alternating optimization (AO) framework is implemented to decompose the nonconvex original problem. In detail, the whole problem is divided into three subproblems to solve. For the nonconvexity of the objective function, successive convex approximation (SCA) is used to transform it, and the penalty function method and difference-of-convex (DC) programming are applied to deal with the nonconvex constraints. Finally, we alternately solve the three subproblems until the entire optimization problem converges. Numerical results show that our proposed algorithm has convergence and better performance than other benchmark algorithms.**

***Index Terms*—Imperfect channel state information (CSI), nonlinear energy harvesting, outage probability criterion, reconfigurable metasurface (RMS), simultaneous wireless information and power transfer (SWIPT).**

I. Introduction

THE RAPID development of wireless communication enables the Internet of Things (IoT) to be utilized in more scenarios, e.g., smart industry, smart medical, and the Internet of Vehicles [1], [2]. Based on the relevant data, it is inferred that the number of IoT devices worldwide will rise to 14.7 billion by 2030 in the future IoT networks [3]. However, IoT devices are usually small in size, which makes the battery capacity often limited and have difficulty in meeting the energy requirements of rich applications in IoT. Therefore, energy management for large-scale IoT devices is a critical issue. Meanwhile, to solve the path loss problem caused by high-frequency communication and ensure that the coverage is not reduced, the number of 5G base stations (BSs) is greatly increased compared with 4G BSs [4]. In addition, massive multiple-input multiple-output (MIMO) requires numerous radio frequency (RF) links to provide support, which will lead to a surge in power consumption and cost. Hence, it is urgent to seek a novel transceiver architecture with low power consumption and low cost.

As a promising technique for energy harvested in the IoT, wireless energy transmission (WET) can convert the received RF signal into electrical energies, which can be well applied to solve the energy management of large-scale IoT devices [5]. Simultaneous wireless information and power transfer (SWIPT) is a valid mode in WET. Specifically, in SWIPT, the user divides the received RF signal into an information decoder (ID) and an energy harvester (EH) through power splitting (PS) or time switching (TS) [6], [7], [8], [9], [10]. With the MIMO technology, SWIPT can also be implemented through antenna switching or spatial switching. In antenna switching, each antenna element is switched dynamically between decoding/rectifying in the antenna domain [11]. In spatial switching, information or energy is transmitted through eigenchannels obtained by the eigenvalue decomposition of the MIMO channel matrix. According to the above-mentioned implementation technology of SWIPT, there have been many studies on the integration of SWIPT into existing communication technology [12], [13], [14]. PS factor and signal autocorrelation matrix are designed jointly to maximize the power harvested in the MIMO channel [12]. Buckley and Heath [13] proposed an energy-receiving architecture under orthogonal frequency division multiplexing (OFDM) system. Under this architecture, the user performs energy harvesting and storage from the cyclic prefix of the signal. SWIPT in nonorthogonal multiple access (NOMA) network was studied in [14], authors consider energy harvested constraint and the Quality-of-Service (QoS) requirement of each user and minimize BS transmit power. For the various implementations of SWIPT mentioned above,

Manuscript received 25 August 2022; revised 3 November 2022; accepted 9 December 2022. Date of publication 13 December 2022; date of current version 7 April 2023. This work was supported in part by the National Key Project under Grant 2020YFB1807700 and Grant 2018YFB1801102; in part by the Shanghai Kewei under Grant 20JC1416502 and Grant 22JC1404000; in part by Pudong under Grant PKX2021-D02; and in part by NSFC under Grant 62071296. *(Corresponding author: Wen Chen.)*

Zhendong Li, Wen Chen, Ziheng Zhang, Qingqing Wu, and Huanqing Cao are with the Department of Electronic Engineering, Shanghai Jiao Tong University, Shanghai 200240, China (e-mail: lizhendong@sjtu.edu.cn; wenchen@sjtu.edu.cn; zhangziheng@sjtu.edu.cn; wu.qq1010@gmail.com; caohuanqing@sjtu.edu.cn).

Jun Li is with the School of Electronic and Optical Engineering, Nanjing University of Science and Technology, Nanjing 210094, China (e-mail: jun.li@njust.edu.cn).

Digital Object Identifier 10.1109/JIOT.2022.3228868

there are also studies comparing these implementations in specific scenarios, especially PS and TS [15], [16], [17]. The authors compare the attainable rate-energy tradeoff in SWIPT-based communication systems for multiple-input single-output (MISO) channel [15] and MIMO channel [16]. Zhou et al. [17] considered the joint optimization of resource allocation and PS in the OFDM system. Jiang et al. [18] approximately obtained the optimal solution to the probability of information and energy coverage for UAVs assisting SWIPT networks and verified it with the Monte Carlo method. All of the above works demonstrate that the performance of the PS scheme is better than that of the TS scheme. However, PS-based SWIPT can solve the energy shortage in IoT devices, but the energy consumption and cost of BSs also need to be considered urgently.

Considering the requirements to reduce the power consumption and cost of the BS, the recently proposed reconfigurable metasurface (RMS) may be a potential solution. RMS also known as reconfigurable intelligent surface (RIS), is an advanced technology that makes it possible to reconfigure wireless channels in wireless communications networks. RMS contains many passive elements with adjustable phase and amplitude. Since RMS is a passive communication equipment, it can only reflect or transmit signal and does not perform signal processing. RMS has the characteristics of low cost and easy deployment and is an environment-friendly communication device [19], [20], [21]. Because of the above advantages of RMS, it has been widely studied in both academia and industry. Specifically, depending on the medium material, RMS is mainly divided into three types: 1) reflective RMS [22], [23], [24], [25]; 2) transmissive RMS [26], [27]; and 3) simultaneously transmitting and reflecting (STAR) RMS [28], [29]. For reflective RMS, it is also called intelligent reflecting surface (IRS) and used to improve the energy efficiency and spectral efficiency of communication networks, and RMS can make the system obtain obvious performance gains in the main communication scenarios. Zhang and Zhang and Yang et al. maximized the communication capacity of the IRS-assisted system in MIMO systems, respectively [22]. Yang et al. [24] applied IRS to physical-layer security to maximize the secret rate. For the transmissive RMS, it can solve the problem of blind coverage in the communication networks. Zeng et al. [26] evaluated the performance of the downlink RIS-assisted communication system and summarized the selection of the optimal working mode of RIS for a specific user location. Zhang et al. [27] proposed an intelligent omni-surface communication system, where transmissive elements adjust the phase of the received signal to improve network coverage. While STAR RMS can split the incident signal into transmitted and reflected signals, helping to achieve full spatial coverage on both sides of the surface. Wu et al. [29] studied the problem of resource allocation in STAR RMS-assisted multicarrier communication networks. In the above researches, RMS is used as a communication auxiliary device for channel reconstruction and performance boost in two modes.

Furthermore, RMS can also be used as a transmitter, which is a very promising research direction. Tang et al. [30] implemented real-time communication of quadrature amplitude modulation (QAM)-MIMO by using reflective RMS and verified the theoretical model. In terms of transmitter design, transmissive RMS has better performance than reflective RMS, which is mainly because of the following two reasons [31], [32], [33], [34]. One of the reasons is that when RMS works in the reflective mode, the user and the feed antenna are located on the same side of the RMS, which makes the incident and the reflected electromagnetic (EM) waves to interfere with each other. Another reason is that the transmissive RMS transceiver can be designed with higher aperture efficiency and operating bandwidth [31]. For the above reasons, applying transmissive RMS to multiantenna transmitter designs is a potential technique in future wireless communications [35].

In view of the two important issues in IoT networks: 1) the limited battery capacity of the devices and 2) the excessive energy consumption of the BSs, we propose a downlink transmission design scheme for SWIPT networks based on the transmissive RMS transceiver. In order to make the design more practical, a nonlinear energy harvesting model is applied to this network model. Compared with the linear energy harvesting model, the nonlinear model has higher energy conversion efficiency [36]. Considering the difficulty of channel estimation in RMS-assisted systems, the channel estimation error matrix is introduced into our model to simulate the impact of imperfect channel state information (CSI). In this article, we aim to maximize the system sum-rate downlink by jointly optimizing RMS transmissive coefficient, power allocation, and PS ratio with the outage probability criterion. Given that the problem formulated is nonconvex, it is necessary to design a reasonable and effective algorithm to solve it. The main contributions of this article can be summarized as follows.

1) We propose a novel transmissive RMS transceiver-enabled SWIPT network architecture, where the RMS is used as transceiver to implement beamforming. Specifically, RMS transmissive coefficient, transmit power allocation, and PS ratio are designed jointly to maximize the system sum-rate. Taking into account the imperfect CSI, we use outage probability to measure QoS and energy harvested requirements, which can demonstrate the robustness of our design. However, it is nontrivial to directly obtain the global optimal solution to this problem since the high coupling of optimization variables.
2) We propose a joint optimization algorithm based on an alternating optimization (AO) framework to solve this formulated robust system sum-rate maximization problem. Specifically, the original problem is first transformed into a tractable problem. Then, the original problem is decoupled into three subproblems with respect to transmit power allocation, PS ratio, and RMS transmissive coefficient to be solved separately. Finally, we alternately optimize the three subproblems till the entire problem converges.
3) Numerical results reveal the superior performance of the proposed algorithm in downlink multiuser

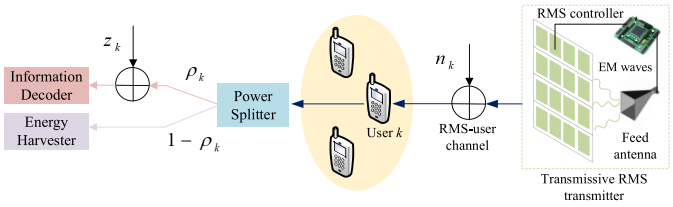

Fig. 1. Transmissive RMS transceiver-enabled SWIPT networks.

SWIPT networks with transmissive RMS as transmitter. Specifically, the algorithm first has good convergence. Second, under the constraints of information and energy harvested requirements based on outage probability criterion, the robust joint optimization algorithm can improve the sum-rate of system compared to other benchmarks under the conditions of a different number of RMS elements, number of users, and maximum transmit power.

The remainder of this article is as follows. In Section II, we delineate the system model and optimization problem formulation in transmissive RMS transceiver-enabled SWIPT networks when considering the nonlinear EH model and the imperfect CSI. Then, in Section III, the proposed robust joint optimization algorithm is elaborated. Section IV reveals the performance superiority of the proposed algorithm compared to other benchmarks. Finally, Section V concludes this article.

Notations: Matrices are represented by bold uppercase letters. Vectors are denoted by bold lowercase letters. Scalars are represented by standard lowercase letters. For a complex-valued scalar x, $|x|$ denotes its absolute value and for a complex-valued vector $\mathbf{x}$, $\|\mathbf{x}\|$ represents the Euclidean norm. For a general matrix $\mathbf{A}$, rank($\mathbf{A}$), $\mathbf{A}^H$, $\mathbf{A}_{m,n}$, and $\|\mathbf{A}\|$ denote its rank, conjugate transpose, m, nth entry, and matrix norm, respectively. For a square matrix $\mathbf{X}$, tr($\mathbf{X}$) and rank($\mathbf{X}$), denote its trace, rank, and $\mathbf{X} \succeq 0$ denotes that $\mathbf{X}$ is a positive semidefinite matrix. $\mathbb{C}^{M\times N}$ represents the $M \times N$ dimensional complex matrix space and j is the imaginary unit. Finally, $\mathcal{CN}(\mu, \mathbf{C})$ denotes the distribution of a circularly symmetric complex Gaussian (CSCG) random vector with mean μ and covariance matrix $\mathbf{C}$, and $\sim$ stands for "distributed as."

II. System Model and Optimization Problem Formulation

A. System Model

As shown in Fig. 1, the system model of transmissive RMS transceiver-enabled SWIPT networks is first introduced and it mainly includes a transmissive RMS transceiver and K users with a single antenna. The transceiver is composed of a transmissive RMS with N elements and a feed antenna. It is worth noting that although we are considering a transmissive RMS transceiver architecture, a portion of the EM waves emitted from the feed antenna will always be reflected. However, we can quantify this part of the reflected EM wave by a certain ratio, so it does not affect the algorithm design of this problem. In this article, for the convenience of analysis, we assume that the EM wave is completely transmitted, i.e., no incident EM waves are reflected. The transmissive RMS is equipped with an intelligent controller which can control the amplitude and phase shift of all transmissive elements. We let $\mathbf{f} = [f_1, \ldots, f_N]^T \in \mathbb{C}^{N\times 1}$ represent the RMS transmissive coefficient vector at the transmitter, where $f_n = \beta_n e^{j\theta_n}$ represents the amplitude and phase shift of the nth element, respectively, which should satisfy

$$|f_n| \le 1 \quad \forall n. \tag{1}$$

The channel from the RMS transceiver to the kth user can be named as the RMS-user channel, and the channel gain can be denoted by $\mathbf{h}_k^H \in \mathbb{C}^{1\times N}$. For ease of analysis, all channels are assumed to be quasi-static flat fading, i.e., $\mathbf{h}_k^H$ is constant within each transmission time T. It is worth noting that the transmissive RMS transmits the signal passively and has no ability to actively send and receive signals. We assume that the communication works in time division duplex (TDD) mode, i.e., the channel estimation is completed in the uplink transmission. Downlink CSI can be obtained according to channel reciprocity. This article assumes that the transmissive RMS transceiver cannot obtain the CSI perfectly, and the specific modeling is explained below.

In this article, we model the array of RMS as a uniform planar array (UPA), which is a more realistic array response, i.e., $N = N_x \times N_z$, N_x and N_z denote the number of elements in the horizontal and vertical directions of the transmissive RMS, respectively. Herein, the RMS-user channel is modeled as a Rice channel model, which can be given by

$$\mathbf{h}_k = \sqrt{\beta\left(\frac{d_k}{d_0}\right)^{-\alpha}}\left(\sqrt{\frac{\kappa}{\kappa+1}}\mathbf{h}_{k,\mathrm{LoS}} + \sqrt{\frac{1}{\kappa+1}}\mathbf{h}_{k,\mathrm{NLoS}}\right) \quad \forall k \tag{2}$$

where β denotes the channel gain when the reference distance $d_0 = 1$ m, α is the path loss exponent between the RMS transceiver and the user, d_k is the distance between RMS transceiver and the kth user. κ denotes the Rician factor, $\mathbf{h}_{k,\mathrm{LoS}}$ represents the LoS component, which can be determined by (3) at the bottom of the page, where θ_k^{AoD} and ϕ_k^{AoD} are the vertical angle and horizontal angle of the Angle-of-Departure (AoD) at the RMS transceiver, respectively. d denotes the spacing between successive antenna elements and λ denotes the carrier wavelength. $\mathbf{h}_{k,\mathrm{NLoS}}$ represents the NLoS component and $[\mathbf{h}_{k,\mathrm{NLoS}}]_{(n_x-1)N_z+n_z} \sim \mathcal{CN}(0,1)$ is the $(n_x-1)N_z+n_z$ element of the vector $\mathbf{h}_{k,\mathrm{NLoS}}$. Accordingly, the signal received by the kth user can be denoted by

$$y_k = \mathbf{h}_k^H \mathbf{f} \sum_{i=1}^{K} \sqrt{p_i} s_i + n_k \quad \forall k \tag{4}$$

where s_i denotes the signal from the RMS transceiver to the ith user, Without loss of generality, we usually assume that

$$\mathbf{h}_{k,\mathrm{LoS}} = \left[1, e^{-j\frac{2\pi}{\lambda}d\sin\theta_k^{\mathrm{AoD}}\cos\phi_k^{\mathrm{AoD}}}, \ldots, e^{-j\frac{2\pi}{\lambda}(N_x-1)d\sin\theta_k^{\mathrm{AoD}}\cos\phi_k^{\mathrm{AoD}}}\right]^T \otimes \left[1, e^{-j\frac{2\pi}{\lambda}d\sin\theta_k^{\mathrm{AoD}}\sin\phi_k^{\mathrm{AoD}}}, \ldots, e^{-j\frac{2\pi}{\lambda}(N_z-1)d\sin\theta_k^{\mathrm{AoD}}\sin\phi_k^{\mathrm{AoD}}}\right]^T \tag{3}$$

it is an independent and identically distributed (i.i.d) CSCG random variable, i.e., $s_i \sim \mathcal{CN}(0,1)$. n_k represents additive white Gaussian noise (AWGN) introduced at the kth user's receiving antenna, and it is also usually set assumed to be i.i.d CSCG variable, i.e., $n_k \sim \mathcal{CN}(0,\sigma_k^2)$. p_k represents the power allocated to the kth user and the following constraints should be satisfied:

$$p_k \geq 0 \quad \forall k \tag{5}$$

and

$$\sum_{k=1}^{K} p_k \leq P_{\max} \tag{6}$$

where $P_{\max}$ is the maximum transmit power of transmissive RMS transceiver.

This article considers transmissive RMS transceiver-enabled SWIPT networks. Specifically, from the received RF signal, each user adopts the PS protocol to coordinate energy harvesting and information decoding, i.e., each user's received signal is divided into the ID and EH by the power splitter. The kth user divide the ρ_k portion of the received signal power to ID and the rest $(1-\rho_k)$ portion to EH. Therefore, the received signal for ID in the downlink of the kth user is denoted by

$$y_k^{\mathrm{ID}} = \sqrt{\rho_k} y_k = \sqrt{\rho_k}\left(\mathbf{h}_k^H \mathbf{f} \sum_{i=1}^{K} \sqrt{p_i} s_i + n_k\right) + z_k \quad \forall k \tag{7}$$

where z_k represents AWGN caused by the ID of the kth user and it is set to be an i.i.d CSCG variable, $z_k \sim \mathcal{CN}(0,\delta_k^2)$. Then, the signal-to-interference plus noise ratio (SINR) of the kth user is denoted by

$$\mathrm{SINR}_k = \frac{\rho_k p_k \left|\mathbf{h}_k^H \mathbf{f}\right|^2}{\rho_k \sum_{i\neq k} p_i \left|\mathbf{h}_k^H \mathbf{f}\right|^2 + \rho_k \sigma^2 + \delta_k^2} \quad \forall k. \tag{8}$$

In addition, for the kth user, the received signal for EH in the downlink can be given by

$$y_k^{\mathrm{EH}} = \sqrt{1-\rho_k} y_k = \sqrt{1-\rho_k}\left(\mathbf{h}_k^H \mathbf{f} \sum_{i=1}^{K} \sqrt{p_i} s_i + n_k\right) \quad \forall k. \tag{9}$$

Accordingly, the power obtained by the kth user for EH is given by

$$p_k^{\mathrm{EH}} = \mathbb{E}\left\{\left|y_k^{\mathrm{EH}}\right|^2\right\} = (1-\rho_k)\left(\sum_{i=1}^{K} p_i \left|\mathbf{h}_k^H \mathbf{f}\right|^2 + \sigma_k^2\right) \quad \forall k. \tag{10}$$

In this article, a more practical nonlinear energy-harvested model is adopted. Hence, the power harvested by the kth user can be expressed as follows:

$$\Psi\left(p_k^{\mathrm{EH}}\right) = \left(\frac{\partial_k}{X_k\left(1+\exp\left(-a_k\left(p_k^{\mathrm{EH}} - b_k\right)\right)\right)} - Y_k\right) \quad \forall k \tag{11}$$

where ∂_k represents the maximum energy harvested of the kth user, a_k and b_k are specific parameters related to the circuit. $X_k = \exp(a_k b_k)/(1+\exp(a_k b_k))$ and $Y_k = \partial_k / \exp(a_k b_k)$. We consider that under normalized time, the energy harvested by the kth user can be given by

$$E_k = \Psi\left(p_k^{\mathrm{EH}}\right) \quad \forall k. \tag{12}$$

Let $\mathbf{\Phi}_k = \mathbb{E}\{\mathbf{h}_k \mathbf{h}_k^H\} = \mathbf{h}_k \mathbf{h}_k^H \in \mathbb{C}^{N\times N}$ represent the channel covariance matrix of the kth user in the downlink.[1] Then, the SINR of the kth user can be expressed by the channel covariance matrix as follows:

$$\mathrm{SINR}_k = \frac{\rho_k p_k \mathrm{tr}(\mathbf{\Phi}_k \mathbf{F})}{\rho_k \sum_{i\neq k} p_i \mathrm{tr}(\mathbf{\Phi}_k \mathbf{F}) + \rho_k \sigma_k^2 + \delta_k^2} \quad \forall k \tag{13}$$

where $\mathbf{F} = \mathbf{f}\mathbf{f}^H \in \mathbb{C}^{N\times N}$ and it should satisfy $\mathrm{rank}(\mathbf{F}) = 1$, $\mathbf{F} \succeq 0$ and $\mathbf{F}_{n,n} \leq 1 \quad \forall n$. In addition, the energy harvested of the kth user is further denoted by

$$E_k = \Psi\left((1-\rho_k)\left(\sum_{i=1}^{K} p_i \mathrm{tr}(\mathbf{\Phi}_k \mathbf{F}) + \sigma_k^2\right)\right) \quad \forall k. \tag{14}$$

To make the model more realistic, we consider that the CSI of the downlink cannot be obtained accurately, i.e., in the case of imperfect CSI. Specifically, the channel covariance matrix is assumed to be expressed as $\mathbf{\Phi}_k + \Delta\mathbf{\Phi}_k$, where $\mathbf{\Phi}_k \in \mathbb{C}^{N\times N}$ denotes the covariance matrix of the estimated channel in the downlink and $\Delta\mathbf{\Phi}_k \in \mathbb{C}^{N\times N}$ is the error matrix corresponding to the estimated error of $\mathbf{\Phi}_k$, which can also be called the uncertainty matrix, because it represents the difference between the estimated value and the true value [37]. Note that $\mathbf{\Phi}_k$ and $\Delta\mathbf{\Phi}_k$ are Hermitian matrices, then the SINR and the energy harvested for the kth user is denoted by

$$\mathrm{SINR}_k = \frac{\rho_k p_k \mathrm{tr}((\mathbf{\Phi}_k + \Delta\mathbf{\Phi}_k)\mathbf{F})}{\rho_k \sum_{i\neq k} p_i \mathrm{tr}((\mathbf{\Phi}_k + \Delta\mathbf{\Phi}_k)\mathbf{F}) + \rho_k \sigma_k^2 + \delta_k^2} \quad \forall k \tag{15}$$

and

$$E_k = \Psi\left((1-\rho_k)\left(\sum_{i=1}^{K} p_i \mathrm{tr}((\mathbf{\Phi}_k + \Delta\mathbf{\Phi}_k)\mathbf{F}) + \sigma_k^2\right)\right) \quad \forall k. \tag{16}$$

Accordingly, the kth user's achievable rate (bps/Hz) is expressed as follows:

$$R_k = \log_2(1 + \mathrm{SINR}_k) \quad \forall k. \tag{17}$$

Since random matrix variable terms are involved in R_k, we take its expectation, which can be defined as $\mathbb{E}\{R_k\}$. However, we cannot use general methods to directly obtain a closed-form expression for the expectation. To solve this problem, we approximate the expectation of the achievable rate by applying Proposition 1 as follows.

Proposition 1: For any a and b, if X is a random variable term or contains a random variable term, the following approximation holds:

$$\mathbb{E}\left\{\log_2\left(1 + \frac{aX}{bX+1}\right)\right\} \approx \mathbb{E}\left\{\log_2\left(1 + \frac{\mathbb{E}\{aX\}}{\mathbb{E}\{bX\}+1}\right)\right\}. \tag{18}$$

Proof: The proof of this formula is similar to the proof of [38, Th. 1] and here the proof is omitted. ■

For the convenience of analysis, we assume that $\Delta\mathbf{\Phi}_k$ is a Hermitian matrix, and the elements on the diagonal are i.i.d. cyclic symmetric real Gaussian random variables with zero

[1] We consider a quasi-static channel model, i.e., during each transmission time duration T, $\mathbf{h}_k$ is a constant. Therefore, we use the instantaneous value of the channel gain to compute the channel covariance matrix instead of the expectation operator.

mean and σ_Φ^2 variance. Other elements are i.i.d. CSCG random variables with zero mean and σ_Φ^2 variance. According to Proposition 1, we can take that the expectation of the kth user's achievable rate as follows:

$$\mathbb{E}\{R_k\} \approx \log_2\left(1+\frac{\rho_k p_k \mathrm{tr}(\mathbf{\Phi}_k\mathbf{F})}{\rho_k\sum_{i\neq k}p_i\mathrm{tr}(\mathbf{\Phi}_k\mathbf{F})+\rho_k\sigma_k^2+\delta_k^2}\right) \quad \forall k. \tag{19}$$

Considering imperfect CSI, the user's SINR is a random variable, which means that we can only express the information and energy harvested requirement with outage probability. We define the information outage probability of the kth user as the probability that its SINR is smaller than the threshold γ_{th}, which can be expressed as (20), shown at the bottom of the page, where $\Pr\{\cdot\}$ is the probability operator. Similarly, energy harvested outage probability is defined as the probability that the energy harvested is lower than the threshold E_{th}, which can be expressed as (21), shown at the bottom of the page.

B. Problem Formulation

Let $\boldsymbol{\rho} = [\rho_1, \ldots, \rho_K]$ and $\mathbf{p} = [p_1, \ldots, p_K]$. We consider that the information outage probability of each user is not greater than ζ_k, and the energy outage probability of each user is not greater than ε_k. By jointly optimizing the PS ratio $\boldsymbol{\rho}$, RMS transmissive coefficient $\mathbf{F}$, and the transmit power allocation $\mathbf{p}$, the expectation of the system sum-rate is maximized. Therefore, the original problem P0 can be expressed as follows:

$$\begin{aligned}
\mathrm{P0}: \max_{\boldsymbol{\rho},\mathbf{p},\mathbf{F}} \ & \sum_{k=1}^{K}\log_2\left(1+\frac{\rho_k p_k \mathrm{tr}(\mathbf{\Phi}_k\mathbf{F})}{\rho_k\sum_{i\neq k}p_i\mathrm{tr}(\mathbf{\Phi}_k\mathbf{F})+\rho_k\sigma_k^2+\delta_k^2}\right) \\
\text{s.t.} \ & p_k \geq 0 \quad \forall k && \text{(22a)}\\
& \sum_{k=1}^{K} p_k \leq P_{\max} && \text{(22b)}\\
& 0 \leq \rho_k \leq 1 \quad \forall k && \text{(22c)}\\
& \Pr\{\mathrm{SINR}_k \leq \gamma_{th}\} \leq \zeta_k \quad \forall k && \text{(22d)}\\
& \Pr\{E_k \leq E_{th}\} \leq \varepsilon_k \quad \forall k && \text{(22e)}\\
& \mathbf{F}_{n,n} \leq 1 \quad \forall n && \text{(22f)}\\
& \mathbf{F} \succeq 0 && \text{(22g)}\\
& \mathrm{rank}(\mathbf{F}) = 1 && \text{(22h)}
\end{aligned}$$

where constraint (22a) and constraint (22b) are the transmit power allocation constraints of transmissive RMS transceiver, constraint (22c) is the PS ratio constraint of each user. To guarantee the QoS of user information and energy harvesting at the same time, constraint (22d) ensures that the information outage probability of each user is not greater than ζ_k and constraint (22e) ensures that the energy harvesting outage probability of each user is not greater than ε_k. Constraints (22f)–(22h) are RMS transmissive coefficient constraints.

As can be observed, the original problem P0 is nonconvex for the following several reasons: First, the highly coupled variables make the objective function nonconcave. In addition, constraints (22d) and (22e) are constraints based on the outage probability criterion, which are difficult to handle directly. Finally, a nonconvex rank-one constraint (22h) is introduced after the RMS transmissive coefficient vector is lifted to a matrix. Therefore, solving this problem is challenging.

III. Robust Joint Optimization Algorithm Design in Transmissive RMS Transceiver-Enabled SWIPT Networks

A. Problem Transformation

Obviously, problem P0 is a nonconvex optimization problem and needs to be transformed into a tractable convex problem. Next, we reformulate the probability constraint (21d) through a statistical model. Herein, $\mathcal{O}_k^{\mathrm{ID}}$ can be rewritten as (23), shown at the bottom of the page. We introduce the auxiliary matrix

$$\tilde{\mathbf{\Phi}}_k = \rho_k p_k \mathbf{\Phi}_k - \rho_k\gamma_{th}\sum_{i\neq k} p_i\mathbf{\Phi}_k \quad \forall k \tag{24}$$

and

$$\Delta\tilde{\mathbf{\Phi}}_k = \rho_k p_k \Delta\mathbf{\Phi}_k - \rho_k\gamma_{th}\sum_{i\neq k} p_i\Delta\mathbf{\Phi}_k \quad \forall k. \tag{25}$$

Then, the information outage probability of the kth user can be given by

$$\mathcal{O}_k^{\mathrm{ID}} = \Pr\left\{\mathrm{tr}\left(\left(\tilde{\mathbf{\Phi}}_k + \Delta\tilde{\mathbf{\Phi}}_k\right)\mathbf{F}\right) \leq \rho_k\gamma_{th}\sigma_k^2 + \gamma_{th}\delta_k^2\right\} \quad \forall k. \tag{26}$$

$$\mathcal{O}_k^{\mathrm{ID}} = \Pr\{\mathrm{SINR}_k \leq \gamma_{th}\} = \Pr\left\{\frac{\rho_k p_k \mathrm{tr}((\mathbf{\Phi}_k+\Delta\mathbf{\Phi}_k)\mathbf{F})}{\rho_k\sum_{i\neq k}p_i\mathrm{tr}((\mathbf{\Phi}_k+\Delta\mathbf{\Phi}_k)\mathbf{F})+\rho_k\sigma_k^2+\delta_k^2} \leq \gamma_{th}\right\} \quad \forall k \tag{20}$$

$$\mathcal{O}_k^{\mathrm{EH}} = \Pr\{E_k \leq E_{th}\} = \Pr\left\{\Psi\left((1-\rho_k)\left(\sum_{i=1}^{K} p_i\mathrm{tr}((\mathbf{\Phi}_k+\Delta\mathbf{\Phi}_k)\mathbf{F}) + \sigma_k^2\right)\right) \leq E_{th}\right\} \quad \forall k \tag{21}$$

$$\mathcal{O}_k^{\mathrm{ID}} = \Pr\left\{\rho_k p_k \mathrm{tr}((\mathbf{\Phi}_k+\Delta\mathbf{\Phi}_k)\mathbf{F}) \leq \rho_k\gamma_{th}\sum_{i\neq k} p_i\mathrm{tr}((\mathbf{\Phi}_k+\Delta\mathbf{\Phi}_k)\mathbf{F}) + \rho_k\gamma_{th}\sigma_k^2 + \gamma_{th}\delta_k^2\right\} \quad \forall k \tag{23}$$

We define a random variable $\chi_k = \mathrm{tr}((\tilde{\mathbf{\Phi}}_k + \Delta\tilde{\mathbf{\Phi}}_k)\mathbf{F}) \quad \forall k$ and an intermediate variable to be optimized $c_k = \rho_k\gamma_{th}\sigma_k^2 + \gamma_{th}\delta_k^2 \quad \forall k$. Since $\tilde{\mathbf{\Phi}}_k$, $\Delta\tilde{\mathbf{\Phi}}_k$, and $\mathbf{F}$ are all Hermitian matrices, the following Proposition 2 can be cited for the probability distribution analysis of χ_k.

Proposition 2: If $\mathbf{X}$ is a random matrix with CSCG random elements with 0 mean and variance σ_x^2, for any deterministic matrix $\mathbf{Y}$, the following formula is established:

$$\mathrm{tr}(\mathbf{YX}) \sim \mathcal{CN}\Big(0, \sigma_{\mathrm{x}}^2\mathrm{tr}\big(\mathbf{YY}^{\mathrm{H}}\big)\Big). \tag{27}$$

According to [39, Proposition 2], we can obtain $\chi_k \sim \mathcal{CN}(\mathrm{tr}(\tilde{\Phi}_k\mathbf{F}), \sigma_{e,k}^2\mathrm{tr}(\mathbf{FF}^H))$, where $\sigma_{e,k}^2$ can be given by

$$\sigma_{e,k}^2 = \rho_k^2 p_k^2\sigma_\Phi^2 + \rho_k^2\gamma_{th}^2\sum_{i\neq k} p_i^2\sigma_\Phi^2 \quad \forall k \tag{28}$$

then

$$\sigma_{e,k}^2 = \rho_k^2\sigma_\Phi^2\left(p_k^2 + \gamma_{th}^2\sum_{i\neq k} p_i^2\right) \quad \forall k. \tag{29}$$

Therefore, the information outage probability of the kth user $\mathcal{O}_k^{\mathrm{ID}}$ can be obtained by (30), shown at the bottom of the page, where $\|\mathbf{F}\|^2 = \mathrm{tr}(\mathbf{FF}^H)$. According to the definition of the error function

$$erf(x) = \frac{2}{\sqrt{\pi}}\int_0^x \exp\big(-u^2\big)du \tag{31}$$

the information outage probability of the kth user can finally be given by

$$\mathcal{O}_k^{\mathrm{ID}} = \frac{1}{2} - \frac{1}{2}erf\left(\frac{\mathrm{tr}\Big(\tilde{\mathbf{\Phi}}_k\mathbf{F}\Big) - c_k}{\sqrt{2}\sigma_{e,k}\|\mathbf{F}\|}\right) \quad \forall k. \tag{32}$$

Thus, constraint (22d) can be rewritten as follows:

$$\frac{1}{2} - \frac{1}{2}erf\left(\frac{\mathrm{tr}\Big(\tilde{\mathbf{\Phi}}_k\mathbf{F}\Big) - c_k}{\sqrt{2}\sigma_{e,k}\|\mathbf{F}\|}\right) \le \zeta_k \quad \forall k. \tag{33}$$

This formula can be converted to

$$\mathrm{tr}\Big(\tilde{\mathbf{\Phi}}_k\mathbf{F}\Big) - c_k \ge \sqrt{2}\sigma_{e,k}\|\mathbf{F}\|erf^{-1}(1-2\zeta_k) \quad \forall k. \tag{34}$$

Similarly, the kth user's energy outage probability $\mathcal{O}_k^{\mathrm{EH}}$ is denoted by (35), shown at the bottom of the page, where $\widehat{\Phi}_k = (1-\rho_k)\sum_{i=1}^K p_i\mathbf{\Phi}_k$, $\Delta\widehat{\Phi}_k = (1-\rho_k)\sum_{i=1}^K p_i\Delta\mathbf{\Phi}_k$ and $\varphi_k = \Psi^{-1}(E_{th}) - (1-\rho_k)\sigma_k^2$. Then, we define a random variable $\varpi_k = \mathrm{tr}((\widehat{\Phi}_k + \Delta\widehat{\Phi}_k)\mathbf{F})$. According to Proposition 2, we can obtain $\varpi_k \sim \mathcal{CN}(\mathrm{tr}(\widehat{\Phi}_k\mathbf{F}), \beta_{e,k}^2\mathrm{tr}(\mathbf{FF}^H))$, where $\beta_{e,k}^2$ can be given by

$$\beta_{e,k}^2 = (1-\rho_k)^2\sum_{i=1}^K p_i{}^2\sigma_\Phi^2 \quad \forall k. \tag{36}$$

Therefore, the kth user's energy outage probability $\mathcal{O}_k^{\mathrm{EH}}$ is obtained by (37), shown at the bottom of the page. Thus, the constraint (22e) can be rewritten as follows:

$$\frac{1}{2} - \frac{1}{2}erf\left(\frac{\mathrm{tr}\Big(\widehat{\Phi}_k\mathbf{F}\Big) - \varphi_k}{\sqrt{2}\beta_{e,k}\|\mathbf{F}\|}\right) \le \varepsilon_k \quad \forall k. \tag{38}$$

This formula can be converted to

$$\mathrm{tr}\Big(\widehat{\Phi}_k\mathbf{F}\Big) - \varphi_k \ge \sqrt{2}\beta_{e,k}\|\mathbf{F}\|erf^{-1}(1-2\varepsilon_k) \quad \forall k. \tag{39}$$

Hence, we can transform problem P0 into problem P1, which can be given by

$$\mathrm{P1}: \max_{\boldsymbol{\rho},\mathbf{p},\mathbf{F}} \sum_{k=1}^K \log_2\left(1 + \frac{\rho_k p_k \mathrm{tr}(\mathbf{\Phi}_k\mathbf{F})}{\rho_k\sum_{i\neq k} p_i\mathrm{tr}(\mathbf{\Phi}_k\mathbf{F}) + \rho_k\sigma_k^2 + \delta_k^2}\right)$$

$$\text{s.t.} \quad p_k \ge 0 \quad \forall k \tag{40a}$$

$$\sum_{k=1}^K p_k \le P_{\max} \tag{40b}$$

$$0 \le \rho_k \le 1 \quad \forall k \tag{40c}$$

$$\mathrm{tr}\Big(\tilde{\mathbf{\Phi}}_k\mathbf{F}\Big) - c_k \ge \sqrt{2}\sigma_{e,k}\|\mathbf{F}\|erf^{-1}(1-2\zeta_k) \quad \forall k \tag{40d}$$

$$\mathrm{tr}\Big(\widehat{\Phi}_k\mathbf{F}\Big) - \varphi_k \ge \sqrt{2}\beta_{e,k}\|\mathbf{F}\|erf^{-1}(1-2\varepsilon_k) \quad \forall k \tag{40e}$$

$$\mathbf{F}_{n,n} \le 1 \quad \forall n \tag{40f}$$

$$\mathbf{F} \succeq 0 \tag{40g}$$

$$\mathrm{rank}(\mathbf{F}) = 1. \tag{40h}$$

After the original problem is transformed, the AO framework can be implemented to decouple problem P1 into three subproblems: 1) RMS transmissive coefficient optimization;

$$\mathcal{O}_k^{\mathrm{ID}} = \Pr\{\chi_k \le c_k\} = \int_{-\infty}^{c_k}\frac{1}{\sqrt{2\pi}\sigma_{e,k}\|\mathbf{F}\|}\exp\left(-\frac{\Big(\chi_k - \mathrm{tr}\Big(\tilde{\mathbf{\Phi}}_k\mathbf{F}\Big)\Big)^2}{2\sigma_{e,k}^2\|\mathbf{F}\|^2}\right)d\chi_k \quad \forall k \tag{30}$$

$$\mathcal{O}_k^{\mathrm{EH}} = \Pr\left\{\Psi\left((1-\rho_k)\left(\sum_{i=1}^K p_i\mathrm{tr}((\mathbf{\Phi}_k + \Delta\mathbf{\Phi}_k)\mathbf{F}) + \sigma_{e,k}^2\right)\right) \le E_{th}\right\} = \Pr\left\{\mathrm{tr}\Big(\Big(\widehat{\Phi}_k + \Delta\widehat{\Phi}_k\Big)\mathbf{F}\Big) \le \varphi_k\right\} \quad \forall k \tag{35}$$

$$\mathcal{O}_k^{\mathrm{EH}} = \Pr\{\varpi_k \le \varphi_k\} = \int_{-\infty}^{\varphi_k}\frac{1}{\sqrt{2\pi}\beta_{e,k}\|\mathbf{F}\|}\exp\left(-\frac{\Big(\varpi_k - \mathrm{tr}\Big(\widehat{\Phi}_k\mathbf{F}\Big)\Big)^2}{2\beta_{e,k}^2\|\mathbf{F}\|^2}\right)d\varpi_k = \frac{1}{2} - \frac{1}{2}erf\left(\frac{\mathrm{tr}\Big(\widehat{\Phi}_k\mathbf{F}\Big) - \varphi_k}{\sqrt{2}\beta_{e,k}\|\mathbf{F}\|}\right) \quad \forall k \tag{37}$$

2) transmit power allocation optimization; and 3) PS ratio optimization. Then, three nonconvex subproblems are transformed into convex subproblems by applying difference-of-convex (DC) programming and successive convex approximation (SCA), respectively. Next, by alternately optimizing these three subproblems to reach convergence, the final RMS transmissive coefficient, transmit power allocation, and PS ratio scheme can be obtained.

B. RMS Transmissive Coefficient Optimization

In this section, we first fix the PS ratio $\boldsymbol{\rho}$ and transmit power allocation $\mathbf{p}$, and optimize the RMS transmissive coefficient $\mathbf{F}$. The objective function can be expressed as (41), shown at the bottom of the page, which is the difference of two concave functions with respect to (w.r.t) $\mathbf{F}$, which are not concave. Herein, we approximate $\bar{g}_k(\mathbf{F})$ linearly by SCA as follows:

$$\begin{aligned}\bar{g}_k(\mathbf{F}) &\le \bar{g}_k\left(\mathbf{F}^r\right)+\mathrm{tr}\left(\left(\nabla_{\mathbf{F}}\bar{g}_k\left(\mathbf{F}^r\right)\right)^H\left(\mathbf{F}-\mathbf{F}^r\right)\right)\\ &\triangleq \bar{g}_k(\mathbf{F})^{ub} \quad \forall k\end{aligned} \tag{42}$$

with

$$\nabla_{\mathbf{F}}\bar{g}_k\left(\mathbf{F}^r\right)=\frac{\rho_k\sum_{i\neq k}p_i\boldsymbol{\Phi}_k^H}{\left(\rho_k\sum_{i\neq k}p_i\mathrm{tr}(\boldsymbol{\Phi}_k\mathbf{F}^r)+\rho_k\sigma_k^2+\delta_k^2\right)\ln 2} \quad \forall k \tag{43}$$

where $\mathbf{F}^r$ represents the value at the rth SCA iteration. Therefore, problem P1 can be approximately expressed as follows:

$$\begin{aligned}\text{P2: }\max_{\mathbf{F}}\ &\sum_{k=1}^{K}\left(g_k(\mathbf{F})-\bar{g}_k(\mathbf{F})\right)\\ \text{s.t. }\ &\mathrm{tr}\left(\tilde{\boldsymbol{\Phi}}_k\mathbf{F}\right)-c_k\ge\sqrt{2}\sigma_{e,k}\|\mathbf{F}\|erf^{-1}(1-2\zeta_k)\quad\forall k &(44a)\\ &\mathrm{tr}\left(\widehat{\Phi}_k\mathbf{F}\right)-\varphi_k\ge\sqrt{2}\beta_{e,k}\|\mathbf{F}\|erf^{-1}(1-2\varepsilon_k)\quad\forall k &(44b)\\ &\mathbf{F}_{n,n}\le 1\quad\forall n &(44c)\\ &\mathbf{F}\succeq 0 &(44d)\\ &\mathrm{rank}(\mathbf{F})=1. &(44e)\end{aligned}$$

Since the constraint (44e) is nonconvex, we consider that apply the DC programming to address this nonconvex rank-one constraint.

Lemma 1: For any square matrix $\mathbf{B}\in\mathbb{C}^{N\times N}$, $\mathbf{B}\succeq 0$ and $\mathrm{tr}(\mathbf{B})>0$, whose rank is one can be equivalently expressed as follows:

$$\mathrm{rank}(\mathbf{B})=1\Rightarrow\mathrm{tr}(\mathbf{B})-\|\mathbf{B}\|_2=0 \tag{45}$$

where $\mathrm{tr}(\mathbf{B})=\sum_{n=1}^{N}\sigma_n(\mathbf{B})$, $\|\mathbf{B}\|_2=\sigma_1(\mathbf{B})$ represents the spectral norm of matrix $\mathbf{B}$, and represents the nth largest singular value of matrix $\mathbf{B}$. On the basis of Lemma 1, rank-one constraint (44e) can be transformed in the optimization problem P2 as follows:

$$\mathrm{rank}(\mathbf{F})=1\Rightarrow\mathrm{tr}(\mathbf{F})-\|\mathbf{F}\|_2=0. \tag{46}$$

Then, a penalty factor ℓ is introduced and the above (46) is added to the objective function of problem P2. Next, it is converted into problem P3, which can be given by

$$\begin{aligned}\text{P3: }\max_{\mathbf{F}}\ &\sum_{k=1}^{K}\left(g_k(\mathbf{F})-\bar{g}_k(\mathbf{F})^{ub}\right)-\ell(\mathrm{tr}(\mathbf{F})-\|\mathbf{F}\|_2)\\ \text{s.t. }\ &\mathrm{tr}\left(\tilde{\boldsymbol{\Phi}}_k\mathbf{F}\right)-c_k\ge\sqrt{2}\sigma_{e,k}\|\mathbf{F}\|erf^{-1}(1-2\zeta_k)\quad\forall k &(47a)\\ &\mathrm{tr}\left(\widehat{\Phi}_k\mathbf{F}\right)-\varphi_k\ge\sqrt{2}\beta_{e,k}\|\mathbf{F}\|erf^{-1}(1-2\varepsilon_k)\quad\forall k &(47b)\\ &\mathbf{F}_{n,n}\le 1\quad\forall n &(47c)\\ &\mathbf{F}\succeq 0 &(47d)\end{aligned}$$

where ℓ represents the penalty factor associated with the rank-one. Because $\|\mathbf{F}\|_2$ is a convex function, problem P3 is still not a convex problem, which can be linearized by using the SCA technique, and its lower bound can be given by

$$\begin{aligned}\|\mathbf{F}\|_2&\ge\left\|\mathbf{F}^r\right\|_2+\mathrm{tr}\left(\mathbf{u}_{\max}\left(\mathbf{F}^r\right)\mathbf{u}_{\max}\left(\mathbf{F}^r\right)^H\left(\mathbf{F}-\mathbf{F}^r\right)\right)\\ &\triangleq(\|\mathbf{F}\|_2)^{lb},\end{aligned} \tag{48}$$

where $\mathbf{u}_{\max}(\mathbf{F}^r)$ denotes the eigenvector corresponding to the largest eigenvalue of the matrix $\mathbf{F}$ at the rth SCA iteration. Thus, problem P3 can be further converted into problem P4 as follows:

$$\begin{aligned}\text{P4: }\max_{\mathbf{F}}\ &\sum_{k=1}^{K}\left(g_k(\mathbf{F})-\bar{g}_k(\mathbf{F})^{ub}\right)-\ell\left(\mathrm{tr}(\mathbf{F})-(\|\mathbf{F}\|_2)^{lb}\right)\\ \text{s.t. }\ &\mathrm{tr}\left(\tilde{\boldsymbol{\Phi}}_k\mathbf{F}\right)-c_k\ge\sqrt{2}\sigma_{e,k}\|\mathbf{F}\|erf^{-1}(1-2\zeta_k)\quad\forall k &(49a)\\ &\mathrm{tr}\left(\widehat{\Phi}_k\mathbf{F}\right)-\varphi_k\ge\sqrt{2}\beta_{e,k}\|\mathbf{F}\|erf^{-1}(1-2\varepsilon_k)\quad\forall k &(49b)\\ &\mathbf{F}_{n,n}\le 1\quad\forall n &(49c)\\ &\mathbf{F}\succeq 0. &(49d)\end{aligned}$$

After the analysis, when the probability of the user's information and energy outage is less than 0.5, the coefficients on the right side of the inequalities of (49a) and (49b) about the matrix $\mathbf{F}$ are positive. In general, the outage probability is not greater than 0.5. The subsequent simulation in this article is set to 0.1, which can satisfy this condition. If the outage probability is set to be greater than 0.5, SCA can be further used to linearize the right-hand side (RHS) of the inequalities of (49a) and (49b) to solve the problem. Therefore, this problem is a semidefinite programming (SDP) problem, which can be efficiently solved by utilizing the CVX toolbox to obtain the RMS transmissive coefficient.

C. Transmit Power Allocation Optimization

In this section, the RMS transmissive coefficient $\mathbf{F}$ and PS ratio $\boldsymbol{\rho}$ are given, and we optimize the transmit power allocation $\mathbf{p}$. The objective function can be denoted by (50), shown at

$$\sum_{k=1}^{K}\left(\log_2\left(\sum_{i=1}^{K}\rho_k p_i\mathrm{tr}(\Phi_k\mathbf{F})+\rho_k\sigma_k^2+\delta_k^2\right)-\log_2\left(\rho_k\sum_{i\neq k}p_i\mathrm{tr}(\Phi_k\mathbf{F})+\rho_k\sigma_k^2+\delta_k^2\right)\right)=\sum_{k=1}^{K}\left(g_k(\mathbf{F})-\bar{g}_k(\mathbf{F})\right)\quad\forall k \tag{41}$$

the bottom of the page. It can be seen that the objective function is the difference of two concave functions w.r.t p_i. Thus, it is a nonconcave function. It can be linearized by SCA, i.e., we perform a first-order Taylor expansion on the second term and (51), shown at the bottom of the page, can be obtained, where p_i^r represents the value at the rth SCA iteration. Hence, problem P1 is transformed as follows:

$$\text{P5: } \max_{\mathbf{p}} \sum_{k=1}^{K}\left(h_k(p_i)-\bar{h}_k(p_i)^{ub}\right)$$
$$\text{s.t. } p_k \geq 0 \quad \forall k \tag{52a}$$
$$\sum_{k=1}^{K} p_k \leq P_{\max} \tag{52b}$$
$$\text{tr}\left(\tilde{\mathbf{\Phi}}_k\mathbf{F}\right)-c_k \geq \sqrt{2}\sigma_{e,k}\|\mathbf{F}\|erf^{-1}(1-2\zeta_k) \quad \forall k \tag{52c}$$
$$\text{tr}\left(\widehat{\Phi}_k\mathbf{F}\right)-\varphi_k \geq \sqrt{2}\beta_{e,k}\|\mathbf{F}\|erf^{-1}(1-2\varepsilon_k) \quad \forall k. \tag{52d}$$

Since the problem is a standard convex optimization problem, we can use CVX toolbox to solve it and obtain the transmit power allocation $\mathbf{p}$.

D. Power Splitting Ratio Optimization

In this section, the PS ratio $\boldsymbol{\rho}$ for each user is optimized when the remaining two sets of variables are fixed. Herein, the objective function can be given by (53), shown at the bottom of the page. Similarly, by using the SCA to linearize the second term in (53), we can obtain (54), shown at the bottom of the page.

Therefore, problem P1 can be transformed into problem P6, which can be given by

$$\text{P6: } \max_{\boldsymbol{\rho}} \sum_{k=1}^{K}\left(f(\rho_k)-\bar{f}(\rho_k)^{ub}\right)$$
$$\text{s.t. } 0 \leq \rho_k \leq 1 \quad \forall k \tag{55a}$$
$$\text{tr}\left(\tilde{\mathbf{\Phi}}_k\mathbf{F}\right)-c_k \geq \sqrt{2}\sigma_{e,k}\|\mathbf{F}\|erf^{-1}(1-2\zeta_k) \quad \forall k \tag{55b}$$
$$\text{tr}\left(\widehat{\Phi}_k\mathbf{F}\right)-\varphi_k \geq \sqrt{2}\beta_{e,k}\|\mathbf{F}\|erf^{-1}(1-2\varepsilon_k) \quad \forall k. \tag{55c}$$

Algorithm 1 Robust Joint Optimization Algorithm in Transmissive RMS-Enabled SWIPT Networks

1: **Input:** $\mathbf{F}^0$, $\mathbf{p}^0$, $\boldsymbol{\rho}^0$, threshold ϵ and iteration index $r=0$.
2: **repeat**
3: Solve the problem P4 to obtain RMS transmissive coefficient $\mathbf{F}^*$.
4: Solve the problem P5 to obtain transmit power allocation $\mathbf{p}^*$.
5: Solve the problem P6 to obtain power splitting ratio $\boldsymbol{\rho}^*$.
6: Update iteration index $r=r+1$.
7: **until** The whole problem satisfies the convergence threshold requirement.
8: **return** RMS transmissive coefficient, transmit power allocation, power splitting ratio.

We can see that this problem is a standard convex optimization problem and can be efficiently solved by utilizing the CVX toolbox.

E. Overall Robust Joint Optimization Algorithm in Transmissive RMS-Enabled SWIPT Networks

In this section, we propose the overall joint RMS transmissive coefficient, transmit power allocation, and PS ratio optimization algorithm and summarize it in Algorithm 1. First, when the transmit power allocation and PS ratio are given, the RMS transmissive coefficient are determined by solving problem P4. We can respectively, solve problems P5 and P6 to obtain the transmit power allocation and PS ratio. At last, the three subproblems are optimized alternately until the entire problem converges.

F. Computational Complexity and Convergence Analysis

1) Computational Complexity Analysis: In each iteration, the computational complexity of the proposed robust joint optimization algorithm is divided into three parts. The first is to solve the SDP problem P4 with complexity $\mathcal{O}(M^{3.5})$ through the interior point method [40]. In addition, the complexity of

$$\sum_{k=1}^{K}\left(\log_2\left(\sum_{i=1}^{K}\rho_k p_i \text{tr}(\Phi_k\mathbf{F})+\rho_k\sigma_k^2+\delta_k^2\right)-\log_2\left(\rho_k\sum_{i\neq k}p_i\text{tr}(\Phi_k\mathbf{F})+\rho_k\sigma_k^2+\delta_k^2\right)\right)=\sum_{k=1}^{K}\left(h_k(p_i)-\bar{h}_k(p_i)\right) \tag{50}$$

$$\bar{h}_k(p_i)\leq\bar{h}_k\left(p_i^r\right)+\frac{\rho_k\text{tr}(\Phi_k\mathbf{F})}{\left(\rho_k\sum_{i\neq k}p_i^r\text{tr}(\Phi_k\mathbf{F})+\rho_k\sigma_k^2+\delta_k^2\right)\ln 2}\left(p_i-p_i^r\right)\triangleq\bar{h}_k(p_i)^{ub}\quad\forall k \tag{51}$$

$$\sum_{k=1}^{K}\left(\log_2\left(\sum_{i=1}^{K}\rho_k p_i \text{tr}(\Phi_k\mathbf{F})+\rho_k\sigma_k^2+\delta_k^2\right)-\log_2\left(\rho_k\sum_{i\neq k}p_i\text{tr}(\Phi_k\mathbf{F})+\rho_k\sigma_k^2+\delta_k^2\right)\right)=\sum_{k=1}^{K}\left(f(\rho_k)-\bar{f}(\rho_k)\right),\forall k \tag{53}$$

$$\bar{f}(\rho_k)\leq\bar{f}\left(\rho_k^r\right)+\frac{\sum_{i\neq k}p_i\text{tr}(\mathbf{\Phi}_k\mathbf{F})+\sigma_k^2}{\left(\rho_k^r\sum_{i\neq k}p_i\text{tr}(\mathbf{\Phi}_k\mathbf{F})+\rho_k^r\sigma_k^2+\delta_k^2\right)\ln 2}\left(\rho_k-\rho_k^r\right)\triangleq\bar{f}(\rho_k)^{ub}\quad\forall k \tag{54}$$

calculating the subgradient through singular value decomposition is $\mathcal{O}(M^3)$. Accordingly, the computational complexity of the first part is at most $\mathcal{O}(M^{3.5})$. Then, both the second part and the third part solve problems P5 and P6 with computational complexity $\mathcal{O}(K^{3.5})$, respectively. Herein, let r be the number of iterations required for the proposed robust joint optimization algorithm to reach convergence, the computational complexity of Algorithm 1 can be expressed as $\mathcal{O}(r(K^{3.5}+M^{3.5}))$.

2) Convergence Analysis: The convergence of the proposed robust joint optimization Algorithm 1 in transmissive RMS-enabled SWIPT networks can be proved as shown later.

Let $\mathbf{F}^r$, $\mathbf{p}^r$, and $\boldsymbol{\rho}^r$ denote the rth iteration solution to problems P4, P5, and P6. The objective function can be expressed as $\mathcal{R}(\mathbf{F}^r, \mathbf{p}^r, \boldsymbol{\rho}^r)$. In step 3 of Algorithm 1, the RMS transmissive coefficient $\mathbf{F}^*$ can be obtained for given $\mathbf{p}^r$ and $\boldsymbol{\rho}^r$. Hence, we have

$$\mathcal{R}\left(\mathbf{F}^r, \mathbf{p}^r, \boldsymbol{\rho}^r\right) \le \mathcal{R}\left(\mathbf{F}^{r+1}, \mathbf{p}^r, \boldsymbol{\rho}^r\right). \tag{56}$$

In step 4 of Algorithm 1, the transmit power allocation $\mathbf{p}^*$ can be obtained when $\mathbf{F}^r$ and $\boldsymbol{\rho}^r$ are given. Herein, we also have

$$\mathcal{R}\left(\mathbf{F}^{r+1}, \mathbf{p}^r, \boldsymbol{\rho}^r\right) \le \mathcal{R}\left(\mathbf{F}^{r+1}, \mathbf{p}^{r+1}, \boldsymbol{\rho}^r\right). \tag{57}$$

Similarly, in step 5 of Algorithm 1, the PS ratio $\boldsymbol{\rho}^*$ can also be obtained when $\mathbf{F}^r$ and $\mathbf{p}^r$ are given. Thus, we have

$$\mathcal{R}\left(\mathbf{F}^{r+1}, \mathbf{p}^{r+1}, \boldsymbol{\rho}^r\right) \le \mathcal{R}\left(\mathbf{F}^{r+1}, \mathbf{p}^{r+1}, \boldsymbol{\rho}^{r+1}\right). \tag{58}$$

Based on the above, we can obtain

$$\mathcal{R}\left(\mathbf{F}^r, \mathbf{p}^r, \boldsymbol{\rho}^r\right) \le \mathcal{R}\left(\mathbf{F}^{r+1}, \mathbf{p}^{r+1}, \boldsymbol{\rho}^{r+1}\right). \tag{59}$$

The above inequality proves that the value of the objective function is monotonic nondecreasing after each iteration of Algorithm 1. In addition, there is an upper bound on the objective function value for problem P1. The above two aspects ensure the convergence performance of Algorithm 1.

IV. Numerical Results

In this section, we demonstrate the effectiveness of the proposed robust joint optimization algorithm in transmissive RMS-enabled SWIPT networks through numerical simulations. In the simulation setting, we consider a 3-D communication network scenario, where the position of RMS transmitter is (0 m, 0 m, 15 m), and $K = 4$ users are randomly distributed in a circle whose center coordinates is (0 m, 0 m, 0 m) with a radius of 50 m. RMS is equipped with $N = 16$ elements. The antenna spacing is set to half the wavelength of the carrier. Meanwhile, we assume that the parameters of all users are the same, i.e., $a_k = 150$, $b_k = 0.024$, and $\xi_k = 24$ mW [41]. Herein, we set $\sigma^2 = -50$ dBm, $\gamma_{th} = -30$ dB, and $E_{th} = -40$ dB in the simulations. The path loss exponent is set as $\alpha = 3$. We set the path loss β to -20 dB when the reference distance is 1 m and set the Rician factor κ to 3 dB. The threshold for algorithm convergence is set as 10^{-3}.

First, the convergence of the proposed algorithm is verified in transmissive RMS-enabled SWIPT networks. Fig. 2 shows the change of system sum-rate with algorithm iterations. It obvious that the sum-rate increases as the number of iterations increases, which verifies our proposed algorithm has good convergence. In addition, we compare the effect of different RMS transmissive element counts on system performance. Considering that the array of RMS is distributed in a UPA with the same number of elements in the horizontal and vertical directions, the number of RMS element is a perfect square. Specifically, we compare the system sum-rate of the proposed algorithm when the number of RMS transmissive elements is 9, 16, and 36. It can be concluded that the larger the number of RMS elements, the upper the system sum-rate.

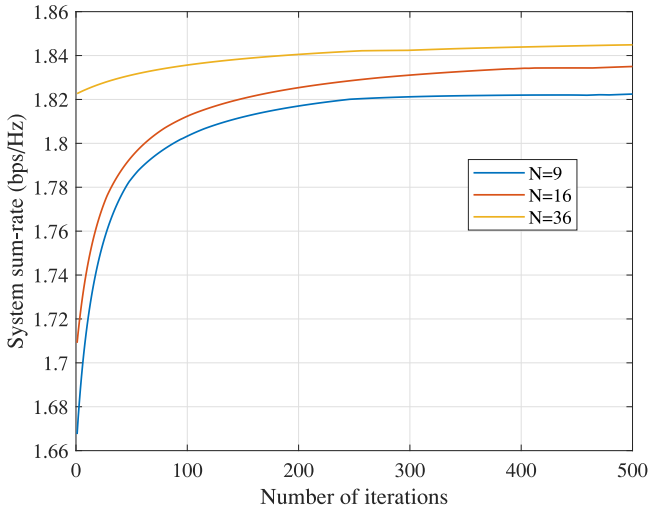

Fig. 2. Convergence behavior of the proposed robust joint optimization algorithm.

In this section, We verify the good performance of the proposed robust joint optimization algorithm in transmissive RMS-enabled SWIPT networks compared with other benchmark algorithms.

1) *Benchmark 1 (RMS-Random-Phase):* In this case, we adopt a random RMS coefficient to deploy RMS and do not optimize its coefficient, i.e., problems P4 and P6 are optimized alternately.
2) *Benchmark 2 (Fixed-Transmit-Power):* In this case, the transmit power is allocated equally to each user, while the RMS transmissive coefficient and PS ratio optimization still use the solution of problems P4 and P6.
3) *Benchmark 3 (Fixed-Power-Splitting-Ratio):* In this case, the PS ratio is regarded as a constant, i.e., $\rho_k = 0.5 \quad \forall k$, and we optimize problems P4 and P5 jointly.

Next, we investigate the relationship between the system sum-rate and the maximum transmit power of the RMS transceiver. As shown in Fig. 3, the system sum-rate increases as the increase of the maximum transmit power of the RMS transceiver, and the performance of our proposed algorithm outperforms all benchmarks, which reflects the advantage of jointly optimizing the RMS transmissive coefficient, transmit power allocation and PS ratio. The performance of benchmark 2 is the worst because it equally allocates the transmit power to each user and does not take advantage of the channel differences of different users. The performance of the system can be

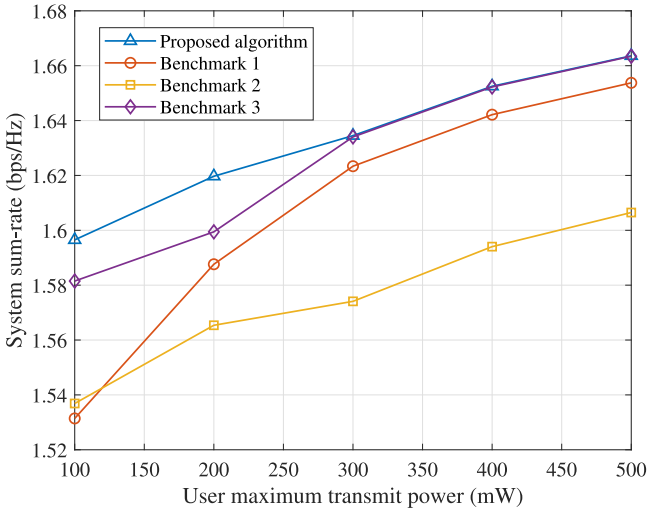

Fig. 3. System sum-rate versus maximum transmit power.

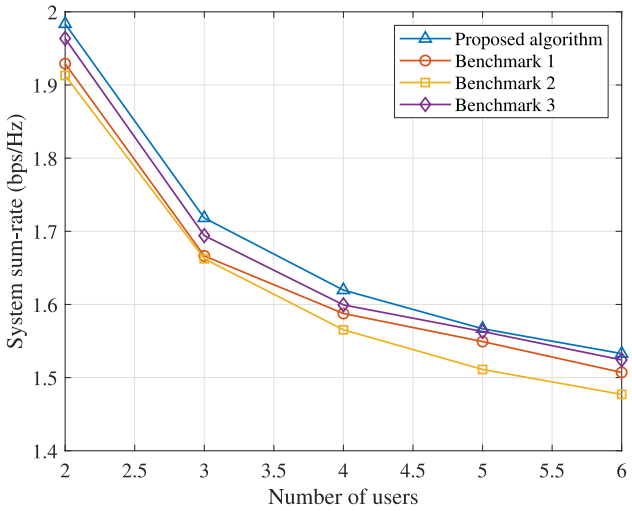

Fig. 5. System sum-rate versus the number of users.

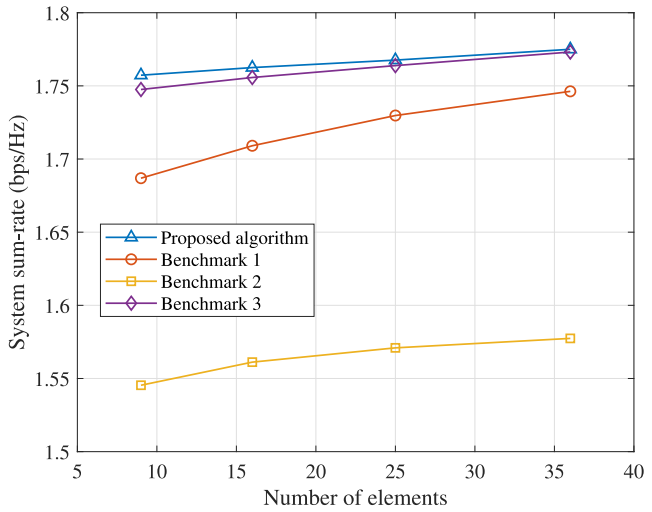

Fig. 4. System sum-rate versus the number of RMS transmissive elements.

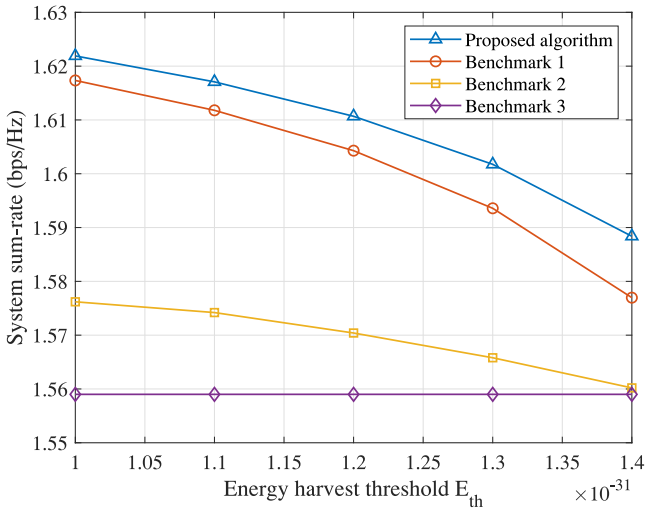

Fig. 6. System sum-rate versus the energy harvested threshold.

improved by allocating more resources to users whose channel quality is better. Compared with benchmark 3, the proposed scheme has similar performance when the transmit power is high, because when the power is high, the constraints of the user's SINR and energy harvested are easier to meet, and the system performance mainly depends on the transmissive RMS coefficient design and transmit power allocation.

Fig. 4 shows the system sum-rate verus the number of RMS transmissive elements. It can be seen that the system sum-rate increases as the number of transmissive RMS element increases for all benchmark algorithms, which is mainly because when the number of transmissive elements increases, the number of reconstructed channels increases, and the channel gain of the receiver increases. This also reflects the performance advantage of the RMS as a low-cost passive component, which improves spatial diversity by increasing the number of RMS elements without requiring additional signal processing. It has a wide range of application in IoT networks. Moreover, the proposed algorithm has obvious performance advantages in different numbers of RMS elements, which reflecting the advantage of the robust joint optimization algorithm.

Then, the system sum-rate versus the number of users is dipicted in Fig. 5. It is obvious that the system sum-rate decreases as the increase of the number of users. This is mainly because we keep the maximum transmit power unchanged. When the number of users increases and the SINR constraints of each user must be satisfied, each user needs to obtain a certain amount of energy, which leads to mutual interference increases and users with better channels have difficulty obtaining more power. Furthermore, our proposed algorithm still outperforms other benchmarks with the same number of users, which indicates our proposed algorithm can better deal with mutual interference.

Fig. 6 shows the system sum-rate versus energy harvested threshold. It is obvious that when the user's energy harvested threshold increases, the system sum-rate decreases. Owing to when the threshold increases, the user needs to obtain a larger power allocation or decrease the PS ratio to meet the constraints of energy harvested, and the achievable rate of each

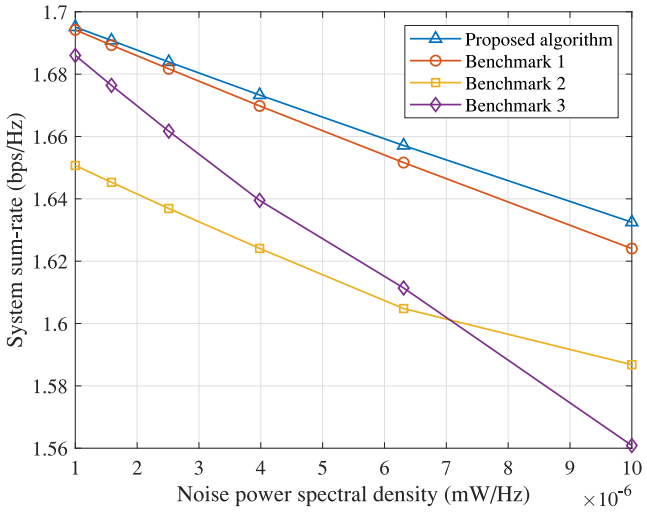

Fig. 7. System sum-rate versus the noise power spectral density.

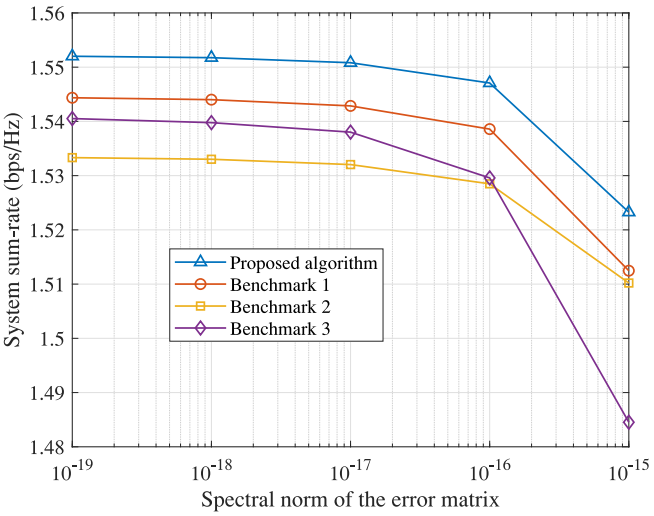

Fig. 8. System sum-rate versus spectral norm of channel error matrix.

user decreases with the decrease of the PS ratio. Therefore, system sum-rate also decreases. While the performance of benchmark 3 remains almost unchanged, this is because we satisfy the constraints by initially setting a reasonable splitting ratio, and the PS ratio will not change in the subsequent alternate optimization process.

Fig. 7 depicts the system sum-rate versus the noise power spectral density. It can be seen that the performance is greatly affected by noise due to the large interference between users in the model considered in this article. As the noise power spectral density increases, the system sum-rate decreases. Compared with other benchmarks, our proposed algorithm has the best performance, and the advantage is more obvious in the environment with larger noise, which shows that our proposed optimization of joint RMS transmissive coefficient, transmit power allocation and PS ratio can be used well in all environments.

Fig. 8 illustrates the variation of our proposed robust joint optimization algorithm and other benchmark algorithms versus different spectral norm of the channel error matrix. The abscissa of Fig. 8 is logarithmic. The increase of channel estimation error will lead to the degradation of system performance. This is mainly because a larger channel estimation error matrix will make the constraints (22d) and (22e) tighter, which will degrade the performance of the system in terms of sum-rate. It is obvious that when the spectral norm of channel error matrix is large, the performance of benchmark 3 decreases sharply. This is because a small PS ratio is set to meet the requirements of constraint (22e) initially, and PS ratio cannot be updated during the alternate optimization process, and the objective function is significantly affected by PS ratio at this time. In fact, perfect CSI cannot be obtained at the transmitter in the practical system, a certain channel estimation error is considered in our model, which is more robust and more conducive for deployment in actual communication networks.

V. Conclusion

In this article, we investigate the system sum-rate maximization problem for transmissive RMS-enabled SWIPT networks. Specifically, RMS transmissive coefficient, transmit power allocation, and PS ratio are jointly designed under the requirements of SINR and energy harvested based on outage probability criterion. First, the problem containing outage probability constraints is transformed into a tractable optimization problem. Owing to nonconvexity of the transformed problem, the AO algorithm based on SCA, DC, and penalty function method is implemented to to handle nonconvexity and solve the problem. Besides, we analyze the complexity of the proposed algorithm and prove its convergence performance. From the numerical results, it can be concluded that our proposed algorithm outperforms other algorithms in terms of system sum-rate, which demonstrate transmissive RMS transceiver is a potential multiantenna technology in the design of future wireless communication networks.

References

[1] F. Al-Turjman and A. Radwan, "Data delivery in wireless multimedia sensor networks: Challenging and defying in the IoT era," *IEEE Wireless Commun.*, vol. 24, no. 5, pp. 126–131, Oct. 2017.

[2] Y. Xu, G. Gui, H. Gacanin, and F. Adachi, "A survey on resource allocation for 5G heterogeneous networks: Current research, future trends, and challenges," *IEEE Commun. Surveys Tuts.*, vol. 23, no. 2, pp. 668–695, 2nd Quart., 2021.

[3] W. Sun, Q. Song, J. Zhao, L. Guo, and A. Jamalipour, "Adaptive resource allocation in SWIPT-enabled cognitive IoT networks," *IEEE Internet Things J.*, vol. 9, no. 1, pp. 535–545, Jan. 2022.

[4] Z. Chu, F. Zhou, Z. Zhu, R. Q. Hu, and P. Xiao, "Wireless powered sensor networks for Internet of Things: Maximum throughput and optimal power allocation," *IEEE Internet Things J.*, vol. 5, no. 1, pp. 310–321, Feb. 2018.

[5] Y. Xu, B. Gu, D. Li, Z. Yang, C. Huang, and K.-K. Wong, "Resource allocation for secure SWIPT-enabled D2D communications with α fairness," *IEEE Trans. Veh. Technol.*, vol. 71, no. 1, pp. 1101–1106, Jan. 2022.

[6] H. Liu, K. J. Kim, K. S. Kwak, and H. V. Poor, "Power splitting-based SWIPT with decode-and-forward full-duplex relaying," *IEEE Trans. Wireless Commun.*, vol. 15, no. 11, pp. 7561–7577, Nov. 2016.

[7] Y. Xu et al., "Joint beamforming and power-splitting control in downlink cooperative SWIPT NOMA systems," *IEEE Trans. Signal Process.*, vol. 65, no. 18, pp. 4874–4886, Sep. 2017.

[8] D. K. Verma, R. Y. Chang, and F.-T. Chien, "Energy-assisted decode-and-forward for energy harvesting cooperative cognitive networks," *IEEE Trans. Cogn. Commun. Netw.*, vol. 3, no. 3, pp. 328–342, Sep. 2017.

[9] J. Tang, A. Shojaeifard, D. K. C. So, K.-K. Wong, and N. Zhao, "Energy efficiency optimization for CoMP-SWIPT heterogeneous networks," *IEEE Trans. Commun.*, vol. 66, no. 12, pp. 6368–6383, Dec. 2018.

[10] Y. Xu, G. Li, Y. Yang, M. Liu, and G. Gui, "Robust resource allocation and power splitting in SWIPT enabled heterogeneous networks: A robust minimax approach," *IEEE Internet Things J.*, vol. 6, no. 6, pp. 10799–10811, Dec. 2019.

[11] I. Krikidis, S. Timotheou, S. Nikolaou, G. Zheng, D. W. K. Ng, and R. Schober, "Simultaneous wireless information and power transfer in modern communication systems," *IEEE Commun. Mag.*, vol. 52, no. 11, pp. 104–110, Nov. 2014.

[12] Z. Chen, Q. Shi, Q. Wu, and W. Xu, "Joint transceiver optimization of MIMO SWIPT systems for harvested power maximization," *IEEE Signal Process. Lett.*, vol. 24, no. 10, pp. 1557–1561, Oct. 2017.

[13] R. F. Buckley and R. W. Heath, "System and design for selective OFDM SWIPT transmission," *IEEE Trans. Green Commun. Netw.*, vol. 5, no. 1, pp. 335–347, Mar. 2021.

[14] Z. Li, W. Chen, Q. Wu, K. Wang, and J. Li, "Joint beamforming design and power splitting optimization in IRS-assisted SWIPT NOMA networks," *IEEE Trans. Wireless Commun.*, vol. 21, no. 3, pp. 2019–2033, Mar. 2022.

[15] C. Shen, W.-C. Li, and T.-H. Chang, "Wireless information and energy transfer in multi-antenna interference channel," *IEEE Trans. Signal Process.*, vol. 62, no. 23, pp. 6249–6264, Dec. 2014.

[16] D. Kudathanthirige, R. Shrestha, and G. A. A. Baduge, "Max–min fairness optimal rate-energy trade-off of SWIPT for massive MIMO downlink," *IEEE Commun. Lett.*, vol. 23, no. 4, pp. 688–691, Apr. 2019.

[17] X. Zhou, R. Zhang, and C. K. Ho, "Wireless information and power transfer in multiuser OFDM systems," *IEEE Trans. Wireless Commun.*, vol. 13, no. 4, pp. 2282–2294, Apr. 2014.

[18] R. Jiang, K. Xiong, P. Fan, L. Zhou, and Z. Zhong, "Outage probability and throughput of multirelay SWIPT-WPCN networks with nonlinear EH model and imperfect CSI," *IEEE Syst. J.*, vol. 14, no. 1, pp. 1206–1217, Mar. 2020.

[19] M. Di Renzo et al., "Reconfigurable intelligent surfaces vs. relaying: Differences, similarities, and performance comparison," *IEEE Open J. Commun. Soc.*, vol. 1, pp. 798–807, 2020.

[20] Z. Li, W. Chen, Q. Wu, H. Cao, K. Wang, and J. Li, "Robust beamforming design and time allocation for IRS-assisted wireless powered communication networks," *IEEE Trans. Commun.*, vol. 70, no. 4, pp. 2838–2852, Apr. 2022.

[21] Y. Xu, H. Xie, Q. Wu, C. Huang, and C. Yuen, "Robust max–min energy efficiency for RIS-aided HetNets with distortion noises," *IEEE Trans. Commun.*, vol. 70, no. 2, pp. 1457–1471, Feb. 2022.

[22] S. Zhang and R. Zhang, "Capacity characterization for intelligent reflecting surface aided MIMO communication," *IEEE J. Sel. Areas Commun.*, vol. 38, no. 8, pp. 1823–1838, Aug. 2020.

[23] H. Cao, Z. Li, and W. Chen, "Resource allocation for IRS-assisted wireless powered communication networks," *IEEE Wireless Commun. Lett.*, vol. 10, no. 11, pp. 2450–2454, Nov. 2021.

[24] H. Yang, Z. Xiong, J. Zhao, D. Niyato, L. Xiao, and Q. Wu, "Deep reinforcement learning-based intelligent reflecting surface for secure wireless communications," *IEEE Trans. Wireless Commun.*, vol. 20, no. 1, pp. 375–388, Jan. 2021.

[25] Y. Xu, Z. Gao, Z. Wang, C. Huang, Z. Yang, and C. Yuen, "RIS-enhanced WPCNs: Joint radio resource allocation and passive beamforming optimization," *IEEE Trans. Veh. Technol.*, vol. 70, no. 8, pp. 7980–7991, Aug. 2021.

[26] S. Zeng et al., "Reconfigurable intelligent surfaces in 6G: Reflective, transmissive, or both?" *IEEE Commun. Lett.*, vol. 25, no. 6, pp. 2063–2067, Jun. 2021.

[27] S. Zhang, H. Zhang, B. Di, Y. Tan, Z. Han, and L. Song, "Beyond intelligent reflecting surfaces: Reflective-transmissive metasurface aided communications for full-dimensional coverage extension," *IEEE Trans. Veh. Technol.*, vol. 69, no. 11, pp. 13905–13909, Nov. 2020.

[28] J. Zuo, Y. Liu, Z. Ding, L. Song, and H. V. Poor, "Joint design for simultaneously transmitting and reflecting (STAR) RIS assisted NOMA systems," *IEEE Trans. Wireless Commun.*, early access, Aug. 19, 2022, doi: 10.1109/TWC.2022.3197079.

[29] C. Wu, X. Mu, Y. Liu, X. Gu, and X. Wang, "Resource allocation in STAR-RIS-aided networks: OMA and NOMA," *IEEE Trans. Wireless Commun.*, vol. 21, no. 9, pp. 7653–7667, Sep. 2022.

[30] W. Tang et al., "MIMO transmission through reconfigurable intelligent surface: System design, analysis, and implementation," *IEEE J. Sel. Areas Commun.*, vol. 38, no. 11, pp. 2683–2699, Nov. 2020.

[31] X. Bai et al., "High-efficiency transmissive programmable metasurface for multimode OAM generation," *Adv. Opt. Mater.*, vol. 8, no. 17, Sep. 2020, Art. no. 2000570.

[32] X. Wan, J. W. Wang, Z. A. Huang, B. Y. Li, Q. Xiao, and T. J. Cui, "Space–time–frequency modulation mechanisms of monochromatic and nonmonochromatic electromagnetic waves on a digital programmable transmission metasurface," *Adv. Funct. Mater.*, vol. 32, no. 13, Mar. 2022, Art. no. 2107557.

[33] B. Liu, Y. He, S.-W. Wong, and Y. Li, "Multifunctional vortex beam generation by a dynamic reflective metasurface," *Adv. Opt. Mater.*, vol. 9, no. 4, Feb. 2021, Art. no. 2001689.

[34] H. Yang et al., "A 1-bit 10×10 reconfigurable reflectarray antenna: Design, optimization, and experiment," *IEEE Trans. Antennas Propag.*, vol. 64, no. 6, pp. 2246–2254, Jun. 2016.

[35] Z. Li, W. Chen, and H. Cao, "Beamforming design and power allocation for transmissive RMS-based transmitter architectures," *IEEE Wireless Commun. Lett.*, vol. 11, no. 1, pp. 53–57, Jan. 2022.

[36] E. Boshkovska, D. W. K. Ng, N. Zlatanov, and R. Schober, "Practical non-linear energy harvesting model and resource allocation for SWIPT systems," *IEEE Commun. Lett.*, vol. 19, no. 12, pp. 2082–2085, Dec. 2015.

[37] B. K. Chalise, S. Shahbazpanahi, A. Czylwik, and A. B. Gershman, "Robust downlink beamforming based on outage probability specifications," *IEEE Trans. Wireless Commun.*, vol. 6, no. 10, pp. 3498–3503, Oct. 2007.

[38] M. Hua, L. Yang, Q. Wu, and A. L. Swindlehurst, "3D UAV trajectory and communication design for simultaneous uplink and downlink transmission," *IEEE Trans. Commun.*, vol. 68, no. 9, pp. 5908–5923, Sep. 2020.

[39] B. K. Chalise and A. Czylwik, "Robust uplink beamforming based upon minimum outage probability criterion," in *Proc. IEEE Global Telecommun. Conf. (GLOBECOM)*, vol. 6, 2004, pp. 3974–3978.

[40] S. Boyd, S. P. Boyd, and L. Vandenberghe, *Convex Optimization*. Cambridge, U.K.: Cambridge Univ. Press, 2004.

[41] Y. Lu, K. Xiong, P. Fan, Z. Ding, Z. Zhong, and K. B. Letaief, "Global energy efficiency in secure MISO SWIPT systems with non-linear power-splitting EH model," *IEEE J. Sel. Areas Commun.*, vol. 37, no. 1, pp. 216–232, Jan. 2019.

Zhendong Li received the B.S. degree in communications engineering from Zhengzhou University, Zhengzhou, China, in 2017, and the master's degree in telecommunication and information systems from Beijing University of Posts and Telecommunications, Beijing, China, in 2020. He is currently pursuing the Ph.D. degree with the Broadband Access Network Laboratory, Department of Electronic Engineering, Shanghai Jiao Tong University, Shanghai, China.

His research interests include reconfigurable intelligent surface, unmanned aerial vehicle communications, space-air-ground (SAG) networks, Internet of Things, and wireless resource management in future wireless networks.

Wen Chen (Senior Member, IEEE) received the B.S. and M.S. degrees from Wuhan University, Wuhan, China, and the Ph.D. degree from the University of Electro-Communications, Chofu, Japan.

He is a tenured Professor with the Department of Electronic Engineering, Shanghai Jiao Tong University, Shanghai, China, where he is the Director of Broadband Access Network Laboratory. He has published more than 120 papers in IEEE journals and more than 120 papers in IEEE Conferences, with citations more than 8000 in google scholar. His research interests include multiple access, wireless AI, and meta-surface communications.

Dr. Chen is the Shanghai Chapter Chair of IEEE Vehicular Technology Society, Editors of IEEE TRANSACTIONS ON WIRELESS COMMUNICATIONS, IEEE TRANSACTIONS ON COMMUNICATIONS, IEEE ACCESS, and IEEE OPEN JOURNAL OF VEHICULAR TECHNOLOGY. He is a Fellow of Chinese Institute of Electronics and the Distinguished Lecturers of IEEE Communications Society and IEEE Vehicular Technology Society.

Ziheng Zhang received the B.S. and master's degrees in communications engineering from the University of Electronic Science and Technology of China, Chengdu, China, in 2015 and 2019, respectively. He is currently pursuing the Ph.D. degree with the Broadband Access Network Laboratory, Department of Electronic Engineering, Shanghai Jiao Tong University, Shanghai, China.

His research interests include reconfigurable intelligent surface and integrated sensing and communication.

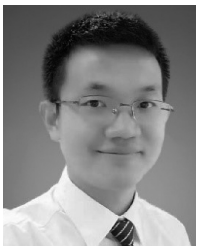

Qingqing Wu (Senior Member, IEEE) received the B.Eng. degree in electronic engineering from South China University of Technology, Guangzhou, China, in 2012, and the Ph.D. degree in electronic engineering from Shanghai Jiao Tong University, Shanghai, China, in 2016.

From 2016 to 2020, he was a Research Fellow with the Department of Electrical and Computer Engineering, National University of Singapore, Singapore. He has coauthored more than 100 IEEE journal papers with 26 ESI highly cited papers and eight ESI hot papers, which have received more than 16 000 Google citations. His current research interest includes intelligent reflecting surface, unmanned aerial vehicle communications, and MIMO transceiver design.

Dr. Wu was the recipient of the IEEE Communications Society Asia–Pacific Best Young Researcher Award and the Outstanding Paper Award in 2022, the IEEE Communications Society Young Author Best Paper Award in 2021, the Outstanding Ph.D. Thesis Award of China Institute of Communications in 2017, the Outstanding Ph.D. Thesis Funding in SJTU in 2016, the IEEE ICCC Best Paper Award in 2021, and the IEEE WCSP Best Paper Award in 2015. He was listed as the Clarivate ESI Highly Cited Researcher in 2022 and 2021, the Most Influential Scholar Award in AI-2000 by Aminer in 2021 and World's Top 2% Scientist by Stanford University in 2020 and 2021. He was the Exemplary Editor of IEEE COMMUNICATIONS LETTERS in 2019 and the exemplary reviewer of several IEEE journals. He serves as an Associate Editor for IEEE TRANSACTIONS ON COMMUNICATIONS, IEEE COMMUNICATIONS LETTERS, IEEE WIRELESS COMMUNICATIONS LETTERS, IEEE OPEN JOURNAL OF THE COMMUNICATIONS SOCIETY, and IEEE OPEN JOURNAL OF VEHICULAR TECHNOLOGY. He is the Lead Guest Editor for IEEE JOURNAL ON SELECTED AREAS IN COMMUNICATIONS on "UAV Communications in 5G and Beyond Networks," and the Guest Editor for IEEE OPEN JOURNAL OF VEHICULAR TECHNOLOGY on "6G Intelligent Communications" and IEEE OPEN JOURNAL OF THE COMMUNICATIONS SOCIETY on "Reconfigurable Intelligent Surface-Based Communications for 6G Wireless Networks." He is the Workshop Co-Chair for IEEE ICC 2019-2022 workshop on "Integrating UAVs into 5G and Beyond," and the Workshop Co-Chair for IEEE GLOBECOM 2020 and ICC 2021 workshop on "Reconfigurable Intelligent Surfaces for Wireless Communication for Beyond 5G." He serves as the Workshops and Symposia Officer of the Reconfigurable Intelligent Surfaces Emerging Technology Initiative and Research Blog Officer of Aerial Communications Emerging Technology Initiative. He is the IEEE Communications Society Young Professional Chair in Asia–Pacific Region.

Huanqing Cao received the B.S. degree in electronic information engineering from Beihang University, Beijing, China, in 2019, and the master's degree from the Broadband Access Network Laboratory, Department of Electronic Engineering, Shanghai Jiao Tong University, Shanghai, China, in 2022.

His research interests include reconfigurable intelligent surface and wireless resource management in future wireless networks.

Jun Li (Senior Member, IEEE) received the Ph.D. degree in electronic engineering from Shanghai Jiao Tong University, Shanghai, China, in 2009.

From January 2009 to June 2009, he worked with the Department of Research and Innovation, Alcatel Lucent Shanghai Bell, Pudong, China, as a Research Scientist. From June 2009 to April 2012, he was a Postdoctoral Fellow with the School of Electrical Engineering and Telecommunications, University of New South Wales, Sydney NSW, Australia. From April 2012 to June 2015, he was a Research Fellow with the School of Electrical Engineering, The University of Sydney, Sydney. Since June 2015, he is a Professor with the School of Electronic and Optical Engineering, Nanjing University of Science and Technology, Nanjing, China. He was a Visiting Professor with Princeton University, Princeton, NJ, USA, from 2018 to 2019. His research interests include network information theory, game theory, distributed intelligence, multiple agent reinforcement learning, and their applications in ultradense wireless networks, mobile edge computing, network privacy and security, and Industrial Internet of Things. He has coauthored more than 200 papers in IEEE journals and conferences, and holds one U.S. patents and more than ten Chinese patents in these areas.

Dr. Li received the Exemplary Reviewer of IEEE TRANSACTIONS ON COMMUNICATIONS in 2018 and the Best Paper Award from IEEE International Conference on 5G for Future Wireless Networks in 2017. He is an Editor of IEEE TRANSACTIONS ON WIRELESS COMMUNICATIONS, and was serving as an editor of IEEE COMMUNICATION LETTERS, and a TPC member for several flagship IEEE conferences.